Atmos. Chem. Phys. Discuss., 12, 4901–4939, 2012
www.atmos-chem-phys-discuss.net/12/4901/2012/
doi:10.5194/acpd-12-4901-2012


Atmospheric Chemistry and Physics Discussions



# A multi-model study of impacts of climate change on surface ozone in Europe

**J. Langner[1], M. Engardt[1], A. Baklanov[2], J. H. Christensen[3], M. Gauss[4], C. Geels[3], G. B. Hedegaard[3], R. Nuterman[2], D. Simpson[4,5], J. Soares[6], M. Sofiev[6], P. Wind[4], and A. Zakey[2]**

[1]Swedish Meteorological and Hydrological Institute, 601 76, Norrköping, Sweden
[2]Danish Meteorological Institute, Lyngbyvej 100, 2100, København Ø, Denmark
[3]Department of Environmental Science, Aarhus University, 4000 Roskilde, Denmark
[4]EMEP MSC-W, Norwegian Meteorological Institute, 0313 Oslo, Norway
[5]Chalmers University of Technology, 412 96 Gothenburg, Sweden
[6]Finnish Meteorological Institute, P.O. Box 503, 00101 Helsinki, Finland

Received: 4 January 2012 – Accepted: 6 February 2012 – Published: 13 February 2012

Correspondence to: J. Langner (joakim.langner@smhi.se)

Published by Copernicus Publications on behalf of the European Geosciences Union.







## Abstract

The impact of climate change on surface ozone over Europe was studied using four offline regional chemistry transport models (CTMs) and one online regional integrated climate-chemistry model (CCM) driven by the same global projection of future climate under the SRES A1B scenario. Anthropogenic emissions of ozone precursors from RCP4.5 for year 2000 were used for simulations of both present and future periods in order to isolate the impact of climate change and to assess the robustness of the result across the different models. The sensitivity of the simulated surface ozone to changes in climate between the periods 2000–2009 and 2040–2049 differs among the models, but the general pattern of change with an increase in southern Europe and decrease in northern Europe is similar across different models. Emissions of isoprene differ substantially between different CTMs ranging from 1.6 to 8.0 $\mathrm{Tg\,yr^{-1}}$ for the current climate, partly due to differences in horizontal resolution of meteorological input data. Also the simulated change in isoprene emissions varies substantially across models explaining part of the different response. Average model changes in summer mean ozone and mean of daily maximum ozone exceed 1 ppb(v) in parts of the land area in southern Europe. Corresponding changes of 95-percentiles of hourly ozone exceed 2 ppb(v) in the same region. Over land areas in northern Europe ensemble mean changes in all these measures are mostly negative.

## 1 Introduction

Despite significant control efforts, air pollution is still a major problem in Europe. During the last decades, target values have been frequently exceeded for ozone ($O_3$), nitrogen dioxide ($NO_2$) and $PM_{10}$ in many European cities, and for $O_3$ also in rural areas (EEA, 2003). Changing patterns of temperature, wind and precipitation will affect the chemistry of air pollutants, their emission, transport, concentration, deposition, exposure and effects (DEFRA, 2007; Andersson et al., 2007; Ellingsen et al., 2008; Hedegaard et al., 2008; Isaksen et al., 2009 and references therein; Royal society, 2008; Hedegaard,





ACPD
12, 4901–4939, 2012



2011). The Nordic countries and the Arctic region are affected by long-range transport of air pollutants from the main source regions in continental Europe. Changes in atmospheric circulation due to climate change can therefore affect future levels of air pollution and deposition (see e.g. AMAP, 2011). Changes in meteorological conditions can also influence local dispersion and deposition conditions to vegetation and thereby influence the effects of both long-range transported and locally emitted air pollutants on human health and ecosystems.

The link between climate change and air pollution in Europe has been assessed in several recent studies using regional CTMs (e.g. Langner et al., 2005; Forkel and Knoche, 2006, 2007; Meleux et al., 2007; Giorgi and Meleux, 2007; Hedegaard et al., 2008; Andersson and Engardt, 2010; Katragkou et al., 2011). Recent model assessments of air quality responding to a changing future climate indicate that some parts of Europe are expected to typically be both warmer and have higher $O_3$ levels. $O_3$ impacts on vegetation and tree growth may increase in a warmer and more humid climate due to changes in growing season and increased stomatal uptake (also in view of rising background $O_3$ concentrations, e.g. Ashmore, 2005). Impaired photosynthesis and biomass accumulation can also lead to reduced carbon sequestration (Sitch et al., 2008).

Regional offline atmospheric chemistry models, CTMs, have been developed for European applications for more than three decades and have been used extensively as tools to provide a basis for decisions on successful emission controls of sulfur, nitrogen and volatile organic compounds in Europe. Despite this long development there is still considerable uncertainty in model predictions of air quality and deposition in Europe due to incomplete scientific knowledge about basic processes and model approximations and insufficient or poor quality input data. Recently a new generation of online integrated climate-chemistry models are being applied for Europe. A number of chemistry-climate models with various levels of online coupling between the chemistry and atmospheric dynamics have been developed to investigate the interactions between climate and air quality (Zhang, 2008). Ultimately fully coupled or "online"





ACPD
12, 4901–4939, 2012



chemistry-climate models should be used to address issues of chemistry-climate interactions (Alapaty et al., 2012). Online methods directly transmit meteorological fields produced by the climate model to a chemistry module and calculate the concentration of climate-relevant tracers. The radiative forcing of these tracers then feeds back into the climate model to affect temperatures and regional circulation. Most online coupled chemistry-climate models are global scale with coarse spatial resolutions (e.g. Emmons et al., 2010). Computational constraints and physical/chemical complexity has prevented the widespread implementation of high-resolution, global coupled chemistry-climate models for long-term climate integrations. To date, only a few regional climate models (RCMs) include online coupling with a range of chemical complexity (Shalapy et al., 2012; Solmon et al., 2006; Zhang et al., 2008).

Several multi-model studies of atmospheric chemistry and long-range transport of air pollution in Europe have been carried out over the last decade (e.g. Vautard et al., 2006, 2007, 2009; van Loon et al., 2007; Cuvelier et al., 2007; Thunis et al., 2007; Colette et al., 2011). These studies have focused on establishing the robustness of model predictions in the present climate. Here we, for the first time, assess the combined uncertainty of predicting the future climate and predicting the atmospheric chemistry and long-range transport of $O_3$ over Europe. This study takes a multi-model approach using four state-of-the-art offline CTMs and one online integrated climate-chemistry model (CCM) to assess the uncertainty/robustness of model predictions of surface $O_3$ over Europe. Here we want to evaluate the sensitivity of simulated surface $O_3$ concentrations to changes in climate. The inclusion of one CCM gives the possibility to analyse the importance of feedbacks of changes in ozone on meteorology. In order to facilitate the analysis of differences between models, and isolate the impacts of meteorological changes, we have chosen to keep anthropogenic emissions at current levels. This choice also enables comparison to earlier studies using single CTMs and a similar setup. A full assessment of future surface $O_3$ concentrations also needs to take into account changes in anthropogenic emissions. This will be the target for future studies using the present model ensemble.





ACPD
12, 4901–4939, 2012



## 2 Methods

The model chain used in this study is illustrated in Fig. 1. The chain starts with the selection of a socio-economic emission scenario which is fed into a global climate model, GCM, to generate a climate projection. The same global climate projection has been the basis for all the simulations performed in this study. The meteorological data from the GCM are then used in an offline hemispheric chemical transport model, CTM, and as boundaries in a regional climate model, RCM. The output from the hemispheric CTM and the RCM is finally used to drive regional offline CTMs for the European domain. Emissions of $O_3$ precursors from the same data base are fed both into the hemispheric CTM and the regional CTMs. In this study we have also utilized one online climate-chemistry model which simulates its own regional climate using the GCM climate and hemispheric CTM output on its boundaries. Two 10-yr time periods were studied, a reference period, 2000–2009, and a future period, 2040–2049.

### 2.1 Climate projection

The climate projection used in this study is from the ECHAM5 model (Roeckner et al., 2006). The RCM used to downscale the GCM projection is the Rossby Centre Regional Climate model version 3, RCA3. Model description and evaluation of different aspects of both current and future climate simulated with RCA3 is given by Samuelsson et al. (2011) and Kjellström et al. (2011). The projection used here is the downscaling named ECHAM5-r3 by Kjellström et al. (2011). The climate projection was derived using the SRES A1B emission scenario (Nakićenović et al., 2000). Six-hourly meteorological output on 21 model levels as well as a range of output variables at the surface were stored from the RCA3 simulations to be used in the offline CTM modelling. The horizontal resolution of RCA3 was $0.44^\circ \times 0.44^\circ$ (ca. $50 \times 50\,\mathrm{km}^2$) on a rotated latitude longitude grid. The climate as downscaled by RCA3 carries on broad features of the climate simulated by the parent GCM. The average temperature change in the period 2000–2040 for the European model domain in the downscaled ECHAM5-r3 is 1.27 °C.





ACPD
12, 4901–4939, 2012



This climate projection has a temperature change until the period 2040–2070 close to the average of an ensemble of 16 different projections downscaled from different GCM runs by RCA3 over Europe (Kjellström et al., 2011).

### 2.2 Emission data

Anthropogenic emissions of nitrogen oxides ($NO_x$), sulfur dioxide ($SO_2$), ammonia ($NH_3$), non-methane hydrocarbons (NMVOC) and carbon monoxide (CO) used in all model simulations were taken from the RCP4.5 scenario (Thomson et al., 2011). The RCP scenarios have been developed as a replacement of the SRES scenarios and are now the basis for current modelling activities in the climate modelling community. In this study we used constant emissions for year 2000 which are actually based on historic information (Lamarque et al., 2010).

Biogenic emissions were implemented differently in the different CTMs (see model descriptions below) and therefore resulted in different emissions. Table 1 summarizes the emissions of isoprene ($C_5H_8$) in the models averaged for the reference and future periods. As can be seen emissions increase with time as the climate gets warmer. In all of the models, changes of temperature and solar radiation drive the $C_5H_8$ emission changes. None of the model accounts for the possible inhibiting effect of $CO_2$ changes discussed by e.g. Arneth et al. (2007). Differences between the models are about a factor of four and illustrate the current large uncertainty in predictions of $C_5H_8$ emissions over Europe. The reliability of the empirically-based methods used in the different models is conditioned by the availability of measurements and there are considerable uncertainties in predicting changes under environmental conditions outside the range used to derive the empirical models (Pacifico et al., 2009).

Apart from differences in methodology differences in the temperature fields used in the model simulation also has a large effect for the simulated isoprene emissions. The temperature fields used in DEHM has a much coarser horizontal resolution compared to the fields derived from the downscaling by the RCM used by the other CTMs. This means that the topography is much smoother in the global data resulting in higher





ACPD
12, 4901–4939, 2012



temperatures in areas with substantial topography. The global model data also shows a broader maximum in southern Europe while the data downscaled by RCA3 put the temperature change more over land (not shown). The average temperature change for the whole grid is larger in the original global data compared to the downscaled version by 0.12 °C

### 2.3 Boundary conditions

Chemical boundary conditions at lateral and top boundaries of the regional models for the following 22 chemical components were provided by the DEHM model; NO, $NO_2$, $O_3$, CO, HCHO, PAN, $HNO_3$, $H_2$, $CH_4$, $CH_3CHO$, $C_2H_6$, $C_5H_8$, $nC_4H_{10}$, o-Xylene, $SO_2$, $NH_3$, $N_2O_5$, $SO_4^{2-}$ (sulphate or sulphuric acid), $NH_4NO_3$, aerosol nitrate, $NH_4HSO_4$, $(NH_4)_2SO_4$. The boundary values taken from DEHM were updated every 6 h and interpolated from the DEHM resolution to the respective geometry of each regional CTM. The online integrated climate-chemistry model used monthly mean boundary conditions from DEHM. To ensure consistency, the offline DEHM model was operated with global ECHAM5-r3 meteorology and also using the global RCP4.5 emissions valid for year 2000. Boundary conditions for other chemical components were specified by each modelling group as their best estimate of the model boundary at ca. 2000.

### 2.4 Model descriptions

#### 2.4.1 The DEHM model

The Danish Eulerian Hemispheric Model (DEHM) is a three-dimensional, Eulerian, CTM (Christensen, 1997; Frohn et al., 2002a, b; Frohn, 2004; Brandt et al., 2012) developed at the Danish National Environmental Research Institute (now Aarhus University). The model domain covers most of the Northern Hemisphere, discretized on a polar stereographic projection, and includes a two-way nesting procedure with several nests with higher resolution over Europe, Northern Europe and Denmark (Frohn et al.,





ACPD
12, 4901–4939, 2012



2002a). In the vertical the model has 20 unevenly distributed layers defined in a terrain following sigma-level coordinate system with top at 100 hPa. The boundary conditions depend on the wind direction. Free boundary conditions are used for areas where mass is transported out of the domain and elsewhere the boundary conditions are set to an annual average background value. For $O_3$, the initial and boundary conditions are based on ozonesonde measurements, interpolated to global monthly 3-D values with a resolution of 4 × 5 degrees (Logan, 1999).

Originally DEHM is based on a chemical scheme by Strand and Hov (1994) which has been extended with a detailed description of the ammonia chemistry through the inclusion of $NH_3$ and related species: ammonium nitrate ($NH_4NO_3$), ammonium bisulphate ($NH_4HSO_4$), ammonium sulphate ($(NH_4)_2SO_4$) and particulate nitrate ($NO_3^-$) formed from nitric acid ($HNO_3$). Furthermore, reactions concerning the aqueous phase production of particulate sulfate have been included. Several of the original photolysis rates as well as rates for inorganic and organic chemistry have been updated with rates from the chemical scheme applied in the EMEP model (Simpson et al., 2003a). The current model version includes 58 photo-chemical compounds (including $NO_x$, $SO_x$, NMVOC, $NH_x$, CO, etc.) and 9 classes of particulate matter ($PM_{2.5}$, $PM_{10}$, TSP, sea-salt <2.5 µm, sea-salt >2.5 µm, smoke from wood stoves, fresh black carbon, aged black carbon, and organic carbon). One of the particle classes, the fraction of sea-salt <2.5 µm, is not yet implemented in the model. DEHM includes 122 chemical reactions. Dry deposition is parameterized similar to the EMEP model (Simpson, 2003b; Emberson, 2000) except for the dry deposition of species on water surfaces where the deposition depends on the solubility of the chemical species and the wind speed (Asman, 1994; Hertel, 1995). Wet deposition includes in-cloud and below-cloud scavenging and is calculated as the product of scavenging coefficients and the concentration. The anthropogenic emissions in the model are based on the RCP4.5 emission scenario and are distributed with height above the surface following patterns depending on the appointed SNAP categories. The emissions from the RCP database have been forced with monthly, weekly and daily cycles. The natural emissions of VOCs (isoprene) are





ACPD
12, 4901–4939, 2012



calculated dynamically in the model according to the IGAC-GEIA biogenic emission model (International Global Atmospheric Chemistry – Global Emission Inventory Activity) (Guenther et al., 1995). Besides isoprene, other naturally emitted VOCs like for example terpenes are not included in the current model version. Natural emissions of $NO_x$ from lightning and soil as well as natural emissions of $NH_3$ from soil/vegetation based on GEIA (Global Emission Inventory Activity) are also included. In the model run used as boundary conditions for the other CTMs (Fig. 1) also natural emissions from biomass burning was included.

### 2.4.2 The DMI modelling framework

In this study the DMI online integrated climate-chemistry model (EnvClimA) has been applied considering the ozone feedback on meteorology. The EnvClimA is a new online climate-chemistry model based on the International Centre for Theoretical Physics (ICTP) regional climate model (RegCM-CHEM4, Shalapy et al., 2012). The updated version of the DMI-EnvClimA model includes aerosol-chemistry-dynamics modules and a new cloud scheme as well as the direct and indirect aerosol effects. EnvClimA is considered as the climate version of Enviro-HIRLAM. Both of DMI-EnvClimA and Enviro-HIRLAM use the same aerosol-chemistry, gas-phase chemistry, feedbacks and cloud scheme.

Tropospheric gas-phase chemistry is integrated into the climate model using the condensed version of the Carbon Bond Mechanism (CBM-Z; Zaveri and Peters, 1999) with lumped species that represent broad categories of organics based on carbon bond structure with a fast Radical Balance Method (RBM). The RegCM model, developed at the Abdus Salam International Centre for Theoretical Physics (ICTP), is a hydrostatic, sigma coordinate model (Pal et al., 2007).

The computationally rapid RBM of Sillman et al. (1991) and Barth et al. (2003) is coupled as a chemical solver to the gas-phase mechanism. Photolysis rates are determined as a function of meteorological and chemical inputs and interpolated from an array of pre-determined values based on the Tropospheric Ultraviolet-Visible Model





ACPD
12, 4901–4939, 2012



(Madronich and Flocke, 1999) with cloud cover corrections by Chang et al. (1987). Cloud optical depths and cloud altitudes from EnvClimA are used in the photolysis calculations, thereby directly coupling the photolysis rates and chemical reactions to meteorological conditions at each model time step. The modelling system is also coupled with aerosol modules and includes direct and indirect aerosol effects. In this study only gas-phases species and their direct effects on meteorological variables were considered.

Dry deposition velocities for 31 gaseous species are calculated from a "big leaf" multiple resistance model (Wesely, 1989; Zhang et al., 2002, 2003) with aerodynamic, quasi-laminar layer, and surface resistance acting in series. The processes assume 20 land-use types and make a distinction between uptake resistance for vegetation, soil, water, snow and ice. In the dry deposition scheme we considered both stomata and non-stomata resistances, which are necessary as the stomata uptake occurs only during the daytime for most chemical species. This leads to a more accurate representation of diurnal variations of dry deposition, a process crucial for climate-chemistry interaction. The aerodynamic resistance is calculated from the model boundary layer stability, wind speed and surface roughness, where a quasi-laminar surface layer is incorporated.

The emission pre-processor code in EnvClimA regrids and interpolates the emissions data to the same model projection and resolution as needed by EnvClimA and unifies the emission units for different inventories. The simulations presented in this study include anthropogenic emissions from RCP4.5 for 2000. Monthly emissions inventories are employed in the model while we note that daily and diurnal variations are not prescribed in the anthropogenic emissions inventories, which may impact the daily minima and maxima ozone concentrations. In the current version of DMI-EnvClimA biogenic isoprene emissions were not considered, because the MEGAN module (Guenther et al., 2006), which is on-line coupled with the land surface model in EnvClimA, was found to overestimate total emitted biogenic isoprene (not shown). Half of the emitted isoprene emission from MEGAN would give reasonable results for $O_3$ concentrations.





ACPD
12, 4901–4939, 2012



We are in processes to improve this issue as future work in the model. The model domain has a horizontal resolution of $50 \times 50$ km and 18 levels in the vertical. Because EnvClimA is a limited-area model, meteorological lateral boundary forcings are required. For present and future simulation such as the one here, initial and lateral boundary conditions for the meteorological fields are provided by global ECHAM5-r3 every six hours. Chemical boundary conditions are provided by DEHM model and were included as monthly averages.

### 2.4.3 The EMEP/MSC-W model

The EMEP MSC-W model is a CTM developed at the EMEP Meteorological Synthesizing Centre – West (EMEP MSC-W) at the Norwegian Meteorological Institute. The model is a development of the 3-D model of Berge and Jakobsen (1998), extended with photo-oxidant and aerosol chemistry (Andersson-Sköld and Simpson, 1999; Simpson et al., 2011). Anthropogenic emissions from European ground-level sources are supplied as gridded annual fields of $NO_x$, $NH_3$, $SO_2$, fine and coarse particulate matter, CO, and NMVOC, modified with monthly and daily factors. The methodology for biogenic emissions used in the EMEP model has undergone a substantial update during 2011, now building upon maps of 115 forest species generated by Köble and Seufert (2001). Emission factors for each forest species and for other land-classes are based upon Simpson et al. (1999), updated with recent literature (see Simpson et al. (2011) and references therein), and driven by hourly temperature and light using algorithms from Guenther et al. (1995). Other emissions include marine emissions of dimethlysulfide, and $SO_2$ from volcanoes. Dry deposition is calculated using a resistance analogy combined with stomatal and non-stomatal conductance algorithms (e.g. Simpson et al., 2003a; Tuovinen et al., 2004), whereas wet deposition uses scavenging coefficients applied to the 3-D rainfall. The model has traditionally been used at $50 \times 50\,km^2$ resolution over Europe, but is flexible with respect to input meteorological data and domain, with applications ranging from $5 \times 5\,km^2$ over the UK (Vieno et al., 2010) to $1^\circ \times 1^\circ$ globally (Jonson et al, 2010a, b). Full details of the EMEP model are given in Simpson et al. (2011).





ACPD
12, 4901–4939, 2012



### 2.4.4 The SILAM model

The modelling tool used in this study is the System for Integrated modeLling of Atmospheric coMposition, SILAM (Sofiev et al., 2006, 2008). Its dynamic core currently includes both Eulerian and Lagrangian advection-diffusion formulations. The Eulerian core used in the current study is based on the transport scheme of Galperin (2000) which incorporates the horizontal diffusion term and is combined with the extended resistance analogy of Sofiev (2002) for vertical diffusion. The system includes a meteorological pre-processor for evaluation of basic features of the boundary layer and the free troposphere using the meteorological fields provided by numerical meteorological models (Sofiev et al., 2010). Physical-chemical modules of SILAM include several tropospheric chemistry schemes, description of primary anthropogenic and natural aerosols and radioactive processes. The removal processes are described via dry and wet deposition. Depending on particle size, mechanisms of dry deposition vary from primarily turbulent diffusion driven removal of fine aerosols to primarily gravitational settling of coarse particles (Slinn and Slinn, 1980; Sofiev et al., 2008). Wet deposition distinguishes between sub- and in-cloud scavenging by both rain and snow (Sofiev et al., 2006; Horn et al., 1987; Smith and Clark, 1989; Jylhä, 1991). The anthropogenic emissions of $NO_x$, $NH_3$, $SO_2$, PM, CO, and NMVOC are provided to the model as gridded annual fields with temporal (monthly, daily and hourly) and vertical description (9 non-regularly spaced levels, with the lowest level thickness of 50 m) according to SNAP sectors. For the current study, emission of two sets of compounds is embedded into the dynamic simulations: biogenic VOC and sea salt (Sofiev et al., 2011). The bio-VOC computations follow the NATAIR model approach and the basic land-use features for the USGS classification, providing isoprene and mono-terpene emissions (currently, only isoprene emission is used in the CB4 mechanism).





ACPD
12, 4901–4939, 2012



### 2.4.5 The MATCH model

The regional off-line Eulerian CTM MATCH is developed at the Swedish Meteorological and Hydrological Institute. The model structure, boundary layer parameterization, advection scheme and numerical treatment is given in Robertson et al. (1999). The chemical scheme in MATCH, based on Simpson et al. (1993), with extensions described in Andersson et al. (2007), considers about 70 species and 130 chemical reactions including the relevant photochemistry for ozone. The dry deposition of gases and aerosols is calculated using a resistance approach depending on land surface type. The wet scavenging is assumed to be proportional to the precipitation intensity for most gaseous and aerosol components. For $O_3$, hydrogen peroxide ($H_2O_2$) and $SO_2$ in-cloud scavenging is calculated assuming Henry's law equilibrium; sub-cloud scavenging is neglected for these species. Important model parameters, such as dry deposition velocities and scavenging coefficients are tabulated in Andersson et al. (2007). Emissions of biogenic isoprene are calculated online in MATCH following Simpson et al. (1995). In the vertical direction, the model domains reach 5–6 km above the surface using 15 model levels. The lowest model layer is ~60 m thick, increasing to ~700 m in layer 15. The temporal resolution of the meteorological input data is six hours, interpolated to one hour inside MATCH; the overall model time step is ten minutes.

## 2.5 Model setup

Table 2 summarizes information on the setup of the different models. Although all models have used the same basic climate projection and the same ozone precursor emissions, three of the models, MATCH, EMEP and SILAM have been run with identical meteorological input data downscaled with RCA3; the same 3-D chemical boundary conditions generated by the DEHM model and the same anthropogenic emission data from RCP4.5. The horizontal grid was also identical and the same as for RCA3 while the vertical discretization was left free to each model. It should be noted that the meteorological input available from the RCA3 downscaling of ECHMA5 lacks some





ACPD
12, 4901–4939, 2012



fields normally used in the default application of the different models, in particular 3-D precipitation, and also has a horizontal grid which is different. Due to computation and storage constraints ozone output was stored every six hours from EnvClimA, while the other models stored ozone output at one hour time resolution.

## 3 Results

### 3.1 Comparison to observations

In Table 3 we compare the performance of the four CTMs and the CCM (EnvClimA) at EMEP stations throughout Europe. The locations of the stations are indicated in Fig. 3. The observations are averaged over the period 1997–2003 while the model data are taken from simulations forced by climate model data covering the reference period, 2000–2009. We have evaluated the models' capabilities to reproduce diurnal average and average of daily maximum $O_3$ concentration over the full year and during summer time (April–September). All comparisons are made with results from the lowest model level in each model. Generally this gives somewhat higher $O_3$ concentrations compared to concentrations extrapolated to e.g. three meter level. Note also that the results for EnvClimA are based on six-hourly data while the results from all other models are based on hourly averages.

In winter EnvClimA has a substantial negative bias for both mean and daily maximum $O_3$, this may be due to the underestimation in the winter temperature (not shown) over north-east Europe and due to feedback of ozone on the meteorological variables, which is included in EnvClimA. For the summer period the bias is reduced and is similar to the DEHM model which also underestimates the daily maximum concentration considerably. The negative bias in EnvClimA is also partly related to the use of six-hourly $O_3$ output data and the omission of biogenic isoprene emissions. SILAM and EMEP overestimate the diurnal average concentration but this overestimation would be reduced if concentrations had been extrapolated to three meter level. The MATCH model





ACPD
12, 4901–4939, 2012



has a slight positive bias for mean concentrations and a negative bias for mean of daily maximum. For all models the bias changes in the negative direction when going from mean to daily maximum values.

The spatial correlation, in all models, is rather poor for the diurnal average concentration but for the average of daily maximum $O_3$ concentration all models display correlation coefficients larger than 0.8 during summer. The online integrated model EnvClimA always features the highest spatial correlation of all models. While the observations are typically taken at ~3 m height, the model data are from the lowest model layers (typically 50 m to 90 m thick, see Table 2) – making the model results not strictly comparable to each other. The DEHM model also features larger horizontal grid squares ($150 \times 150\,km^2$) than the other models – which all operate on a horizontal grid of ca. $50 \times 50\,km^2$.

Figure 2 shows the seasonal cycle of simulated monthly-mean (24 h average) $O_3$ concentrations at EMEP sites in Europe averaged over the reference period 2000–2009 compared to observations averaged over the period 1997–2003. The average seasonal variation of the stations in each quadrant of the simulation domain is shown. Station locations are indicated in Fig. 4. All models show a clear seasonal variation, in line with the observations. Most models also reproduce the broad summer maximum in the south and the spring peak in the north. The positive bias in SILAM and EMEP (cf. Table 3) is most pronounced in the north-western and south-eastern part of the domain. SILAM consequently overestimates average $O_3$ during summer and autumn throughout the domain. Due to the winter temperature bias in north-east Europe discussed above, EnvClimA underestimate concentrations in this area, especially during the winter half of the year. For the stations further south the seasonal variation in EnvClimA is better. Incidentally, MATCH and DEHM feature similar temporal and spatial variations, with overestimations of average $O_3$ concentrations during summer and autumn in the north-western part of the domain and underestimations in the south-western part of the domain during all seasons except summer.





ACPD
12, 4901–4939, 2012



### 3.2 Current situation

Figure 3 shows summer time (April–September) diurnal average $O_3$ concentration in the lowest model layer, as simulated by the five models. The general features, with higher $O_3$ concentrations in the south, especially over the Mediterranean Sea, are evident in all models. MATCH and EMEP have more pronounced differences between $O_3$ over land and sea than the other models. MATCH features the lowest concentrations in southern Europe, including the Mediterranean Sea. EnvClimA features the lowest concentration in north-east Europe. In SILAM most land areas of continental Europe feature 10-yr average summer time concentrations in excess of 45 ppb(v), and parts of northern Italy have summer-average concentrations larger than 55 ppb(v).

Figure 4 shows modelled summer time averages of daily maximum $O_3$ concentrations across Europe. In the evaluation above, both SILAM and EMEP performed very well for this measure, with absolute biases of ~1 % and spatial correlations of 0.85 or higher. In Fig. 4 SILAM features higher values over land while EMEP displays higher values over water. EnvClimA displays a zonal behaviour of average daily maximum concentrations while DEHM, as expected, shows the smoothest variation with high daily maximum concentrations over Italy and adjacent areas of the Mediterranean Sea. MATCH, on the other hand, shows a patchy picture, indicating shorter residence time of high $O_3$ and/or strong effects of local processes which are not present to the same extent in the other models.

### 3.3 Climatically induced changes in ozone concentrations

Figure 5 shows the modelled change in average summer time $O_3$ concentration from the reference period to the future period. Note that the anthropogenic emissions were identical during the two periods to isolate the change in surface $O_3$ due to climate change. Most models simulate increase of surface $O_3$ in southern Europe and decreasing $O_3$ concentrations in northern Europe. EnvClimA – using downscaling with a different regional climate model and online coupling – features increasing average $O_3$ also in northern Europe. All models, and MATCH in particular, display increasing





ACPD
12, 4901–4939, 2012



average $O_3$ concentrations in the North Atlantic east of Iceland. This area coincides with a co-located region of particularly pronounced temperature increase over this period (not shown). The reason for the $O_3$ increase is therefore related to both the locally increasing temperatures – affecting the $O_3$ chemistry – and to a shift in the average wind direction in the area from south-west to a more southerly direction (not shown) which results in a shift of the area influenced by reduced surface $O_3$ concentrations due to dry deposition over Iceland. MATCH is the only model that features decreasing $O_3$ concentrations over the Mediterranean Sea in a future climate. This could be caused by a relatively higher sensitivity in MATCH of $O_3$ losses through photolysis and reaction with water vapour.

The hemispheric model DEHM shows the largest climate induced increase of surface $O_3$ concentrations of all models. The increase in surface $O_3$ in DEHM is also centred on southern Italy and the Balkans, whereas the other models place the maximum impact in Northern Italy and central Europe. This is partly due to a larger temperature increase in the global model data used to drive the DEHM model and the resolution effect on isoprene emissions discussed above. MATCH displays much more details in southern Europe with, for example, areas of the southern Iberian Peninsula also showing increasing average $O_3$ concentrations. The EMEP model shows the least sensitivity of surface $O_3$ concentration to climate change. In the EMEP model the increase in average summertime $O_3$ concentration barely reaches 1 ppb(v) in a few grid-cells. In MATCH large parts of Spain, Italy and the Balkans get $O_3$ increases larger than 1 ppb(v) while in DEHM a significant part of south-eastern Europe gets summer mean $O_3$ increases larger than 2 ppb(v). MATCH and EMEP also calculate significant decreases of average $O_3$ in the N-E part of the domain (i.e. north Norway, Sweden, Finland and north-western Russia). Figure 5 also includes the average results for the MATCH, EMEP and SILAM models. Since these models used identical input data this panel shows the average sensitivity to climate change for these models. The ensemble mean change of mean $O_3$ for these three models exceed 1 ppb(v) in parts of the land area in southern Europe.





ACPD
12, 4901–4939, 2012



The change in summer average daily maximum $O_3$ concentration is shown in Fig. 6. While the absolute values of the changes are larger than in the case of the average concentrations, the spatial patterns are similar. All models display a patchier pattern than in the case of the average concentrations, but MATCH stands out with a far more varied response than the other models. For MATCH this is mainly caused by the coupling of stomatal uptake of $O_3$ to soil moisture, an effect that is not included in the other models. MATCH is also still the only model featuring decreasing daily maximum $O_3$ concentrations over the Mediterranean Sea in a future climate. The ensemble mean change of summer daily maximum $O_3$ for the EMEP, SILAM and MATCH models exceed 1 ppb(v) in parts of the land area in southern Europe.

Figure 7 shows the change in April-September 95-percentile of hourly $O_3$ concentrations averaged for the reference compared to the future period. DEHM again stands out with the largest increase of all models while EMEP features the lowest increase. Although MATCH is the only model simulating increase in the 95-percentile of $O_3$ of more than 2 ppb(v) in southern Spain, all models agree that the increase in 95-percentile is more extended than the change in daily maximum concentrations. Apart from MATCH, which still simulates substantial $O_3$ decreases in northern Europe and over parts of the Mediterranean Sea, all models simulate a more widespread increase in the higher percentiles of hourly $O_3$ concentrations over Europe in a future climate indicating that climate impacts on $O_3$ could be especially important in connection with extreme summer events such as experienced in summer 2003. The ensemble mean change of April-September 95-percentile of hourly $O_3$ concentrations for the EMEP, SILAM and MATCH models exceed 2 ppb(v) in parts of the land area in southern Europe.

## 4 Discussion

The simulated sensitivity of surface $O_3$ to changes in climate can be compared to results from earlier studies. Katragkou et al. (2011) found a lower sensitivity for summer mean $O_3$ in the period 2041–2050 compared to 1991–2000 than we see here. In parts





ACPD
12, 4901–4939, 2012



of southern Europe the change was even reversed with decreasing concentrations. Several other studies on the other hand (e.g. Meleux et al., 2007; Forkel and Knoche, 2006, 2007; Hedegaard et al., 2008; Andersson and Engardt, 2010) simulate larger changes than shown here, but in all these cases the climate projections used were based on the SRES A2 scenario which gives a stronger climate change signal. The time span over which the changes were evaluated were also up to twice as long as the 40-yr period used in this study.

The change in surface ozone caused by climate change should also be related to changes due to anticipated changes in European precursor emissions. In an earlier study using the EMEP model driven by climate data from HadCM3 and SRES A1B, downscaled by HIRHAM to $25 \times 25\,km^2$ resolution, Nyíri et al. (2010) found that the increase in daily maximum $O_3$ from the 2000's to the 2050's due to climate change is overridden by changes in European $O_3$ precursor emissions.

Using a slightly different setup of the DEHM model compared to the present study, Hedegaard (2011) found that using temporal evolution of $O_3$ precursor emission according to RCP4.5 resulted in larger changes in $O_3$ compared to the changes imposed by climate change alone between 1990–1999 and 2090–2099. The relative impact was, however, not uniform with emission changes dominating over climatically induced changes in North and South Europe. In central Europe the impact on surface $O_3$ was larger from changes in climate than changes in emissions. Engardt et al. (2009) assessed changes in surface $O_3$ and AOT40 from 2004 to 2020. They concluded that emission reductions would have a large beneficial impact on near surface $O_3$ across Europe. Changes in AOT40 due to likely emission reductions were always larger than changes imposed by climate change. In the northern part of Europe and along the Atlantic coast, changes in AOT40 following increased hemispheric $O_3$ concentrations and climate change almost counterbalanced the decrease in AOT40 due to pan-European emission reductions.





ACPD
12, 4901–4939, 2012



## 5 Conclusions

We have studied the impact of climate change on surface $O_3$ over Europe using four different CTMs and one CCM and the same global projection of future climate under the SRES A1B scenario. The following conclusions can be drawn:

1. Model simulations using climate model output are able to capture major features of the observed distribution of surface $O_3$ over Europe.

2. The sensitivity of the simulated surface $O_3$ to changes in climate differ among models, but the general pattern of change with an increase in southern Europe and decrease in northern Europe is similar across different models for the chosen climate projection, in particular for the subset of models using meteorological data downscaled using the same regional climate model.

3. Emissions of isoprene differ substantially between different CTMs ranging from 1.6 to 8.0 $Tg\,yr^{-1}$ for the current climate. Also the simulated change in isoprene emissions varies substantially across models. Differences in horizontal model resolution and corresponding horizontal resolution in temperature fields are important factors contributing to these differences.

4. Ensemble mean changes between the periods 2000–2009 and 2040–2049 in summer (April–September) mean $O_3$ and mean of daily maximum $O_3$ exceed 1 ppb(v) in parts of the land area in southern Europe assuming no changes in anthropogenic air pollution emissions. Corresponding changes of 95-percentiles of hourly $O_3$ exceed 2 ppb(v) in the same region. In northern Europe ensemble mean changes in all these measures are mostly negative, although the area with decreasing concentrations is smaller for the higher percentiles indicating that climate impacts on $O_3$ could be especially important in connection with extreme summer events.





ACPD
12, 4901–4939, 2012



5. In general, changes in surface $O_3$ due to climate change presented here are much smaller than what can be expected from anthropogenic emission reductions over the same time period from previous studies.

*Acknowledgements.* This study was supported by the Nordic Council of Ministers (EnsCLIM project no: KoL-10-04), the EU projects ECLAIRE (project no: 282910), MEGAPOLI (no: 212520), TRANSPHORM (no: 243406), Swedish Environmental Protection Agency through the research programme CLEO – Climate Change and Environmental Objectives as well as EMEP under UNECE.

## References

Alapaty, K., Mathur, R., Pleim, J., Hogrefe, Ch., Rao, S. T., Ramaswamy, V., Galmarini, S., Schaap, M., Vautard, R., Makar, P., Baklanov, A., Kallos, G., Vogel, B., and Sokhi, R.: New Directions: Understanding Interactions of Air Quality and Climate Change at Regional Scales,Atmos. Environ., 49, 419–421, doi:10.1016/j.atmosenv.2011.12.016, 2012.

AMAP: AMAP Assessment 2011: Mercury in the Arctic. Arctic Monitoring and Assessment Programme (AMAP), Oslo, Norway, xiv+193 pp., 2011.

Andersson, C. and Engardt, M.: European ozone in a future climate – The importance of changes in dry deposition and isoprene emissions, J. Geophys. Res., 115, D02303, doi:10.1029/2008JD011690, 2010.

Andersson, C., Langner, J., and Bergström, R.: Interannual variation and trends in air pollution over Europe due to climate variability during 1958-2001 simulated with a regional CTM coupled to the ERA40 reanalysis, Tellus B, 59, 77–98, 2007.

Andersson-Sköld, Y. and Simpson, D.: Comparison of the chemical schemes of the EMEP MSC-W and IVL photochemical trajectory models, Atmos. Environ., 33, 1111–1129, doi:10.1016/s1352-2310(98)00296-9, 1999.

Arneth, A., Miller, P. A., Scholze, M., Hickler, T., Schurgers, G., Smith, B., and Prentice, I. C.: $CO_2$ inhibition of global terrestrial isoprene emissions: Potential implications for atmospheric chemistry, Geophys. Res. Lett., 34, L18813, doi:18810.11029/12007GL030615, 2007.

Ashmore, M.: Assessing the Future Global Impacts of Ozone on Vegetation, Plant Cell Environ., 28, 949–964, 2005.





ACPD

12, 4901–4939, 2012



Asman, W. A. H., Sørensen, L. L., Berkowicz, R., Granby, K., Nielsen, H., Jensen, B., Runge, E., Lykkelund, C., Gryning, S. E., and Sempreviva, A. M.: Dry deposition processes, Danish Environmental Protection Agency, Marine Research, 35, Copenhagen, Denmark, 199 pp., 1994.

Barth, M. C., Sillman, S., Hudman, R., Jacobson, M. Z., Kim, C.-H., Monod, A., and Liang, J.: Summary of the cloud chemistry modeling intercomparisons: Photochemical box model simulation, J. Geophys. Res., 108, 4214, doi:10.1029/2002JD002673, 2003.

Berge, E. and Jakobsen, H. A.: A regional scale multi-layer model for the calculation of long-term transport and deposition of air pollution in Europe, Tellus B, 50, 205–223, doi:10.1034/j.1600-0889.1998.t01-2-00001.x, 1998.

Brandt, J., Silver, J. D., Christensen, J. H., Frohn, L. M., Geels, C., Gross, A., Hansen, A. B., Hansen, K. M., Hedegaard, G. B., Skjøth, C. A., Villadsen, H., and Zare, A.: An integrated model study for Europe and North America using the Danish Eulerian Hemispheric Model with focus on intercontinental transport of air pollution Atmos. Environ., doi:10.1016/j.atmosenv.2012.01.011, in press, 2012.

Christensen, J. H.: The Danish Eulerian Hemispheric Model – a Three-Dimensional Air Pollution Model Used for the Arctic, Atmos. Environ., 31, 4169–4191, 1997.

Chang, J. S., Brost, R. A., Isaksen, I. S. A., Madronich, S., Middleton, P., Stockwell, W. R., and Walcek, C. J.: A three-dimensional eulerian acid deposition model: physical concepts and formulation, J. Geophys. Res., 92, 14681–14700, 1987.

Colette, A., Granier, C., Hodnebrog, Ø., Jakobs, H., Maurizi, A., Nyiri, A., Bessagnet, B., D'Angiola, A., D'Isidoro, M., Gauss, M., Meleux, F., Memmesheimer, M., Mieville, A., Rouïl, L., Russo, F., Solberg, S., Stordal, F., and Tampieri, F.: Air quality trends in Europe over the past decade: a first multi-model assessment, Atmos. Chem. Phys., 11, 11657–11678, doi:10.5194/acp-11-11657-2011, 2011.

Cuvelier, C., Thunis, P., Vautard, R., Amann, M., Bessagnet, B., Bedogni, M., Berkowicz, R., Brandt, J., Brocheton, F., Builtjes, P., Carnavale, C., Coppalle, A., Denby, B., Douros, J., Graf, A., Hellmuth, O., Hodzic, A., Honore, C., Jonson, J. E., Kerschbaumer, A., de Leeuw, F., Minguzzi, E., Moussiopoulos, N., Pertot, C., Peuch, V. H., Pirovano, G., Rouil, L., Sauter, F., Schaap, M., Stern, R., Tarrason, L., Vignati, E., Volta, M., White, L., Wind, P., and Zuber, A.: CityDelta: A model intercomparison study to explore the impact of emission reductions in European cities in 2010, Atmos. Environ., 41, 189–207, 2007.

DEFRA: Air quality and climate change: A UK perspective. DEFRA publications, available at:





ACPD

12, 4901–4939, 2012



http://www.defra.gov.uk/environment/airquality/aqeg, 2007.
EEA: Air pollution in Europe 1990–2000, Topic report No 4/2003, European Environment Agency, Copenhagen, 2003.
Emberson, L., Simpson, D., Tuovinen, J.-P., Ashmore, M. R., and Cambridge, H. M.: Towards a model of ozone deposition and stomatal uptake over Europe, EMEP MSC-W Note 6/2000, 2000.
Emmons, L. K., Walters, S., Hess, P. G., Lamarque, J.-F., Pfister, G. G., Fillmore, D., Granier, C., Guenther, A., Kinnison, D., Laepple, T., Orlando, J., Tie, X., Tyndall, G., Wiedinmyer, C., Baughcum, S. L., and Kloster, S.: Description and evaluation of the Model for Ozone and Related chemical Tracers, version 4 (MOZART-4), Geosci. Model Dev., 3, 43–67, doi:10.5194/gmd-3-43-2010, 2010.
Engardt, M., Bergström, R., and Andersson, C.: Climate and emission changes contributing to changes in near-surface ozone in Europe over the coming decades: Results from model studies, Ambio, 38, 452–458, 2009.
Ellingsen, K., Gauss, M., Van Dingenen, R., Dentener, F. J., Emberson, L., Fiore, A. M., Schultz, M. G., Stevenson, D. S., Ashmore, M. R., Atherton, C. S., Bergmann, D. J., Bey, I., Butler, T., Drevet, J., Eskes, H., Hauglustaine, D. A., Isaksen, I. S. A., Horowitz, L. W., Krol, M., Lamarque, J. F., Lawrence, M. G., van Noije, T., Pyle, J., Rast, S., Rodriguez, J., Savage, N., Strahan, S., Sudo, K., Szopa, S., and Wild, O.: Global ozone and air quality: a multi-model assessment of risks to human health and crops, Atmos. Chem. Phys. Discuss., 8, 2163–2223, doi:10.5194/acpd-8-2163-2008, 2008.
Forkel, R. and Knoche, R.: Regional climate changes and its impacts on photooxidant concentrations in southern Germany: Simulations with a coupled regional climate-chemistry model, J. Geophys. Res., 111, D12302, doi:10.1029/2005JD006748, 2006.
Forkel, R. and Knoche, R.: Nested regional climate-chemistry simulations for central Europe, C. R. Geosci., 339, 734–746, doi:10.1016/j.crte.2007.09.018, 2007.
Frohn, L. M.: A study of long-term high-resolution air pollution modelling, Ministry of the Environment, National Environmental Research Institute, Roskilde, Denmark, 444 pp., 2004.
Frohn, L. M., Christensen, J. H., and Brandt, J.: Development and testing of numerical methods for two-way nested air pollution modelling, Phys. Chem. Earth., 27, 1487–1494, 2002a.
Frohn, L. M.: Development of a high-resolution nested air pollution model – The numerical approach, J. Comput. Phys. Part B, 179, 68–94, 2002b.
Galperin, M. V.: The Approaches to Correct Computation of Airborne Pollution Advection, in:





ACPD
12, 4901–4939, 2012



Problems of Ecological Monitoring and Ecosystem Modelling, vol. XVII, Gidrometeoizdat, St. Petersburg, 54–68, 2000 (in Russian).
Giorgi, F. and Meleux, F.: Modelling the regional effects of climate change on air quality, C. R. Geoscience, 339, 721–733, 2007.
Guenther, A., Hewitt, C., Erickson, D., Fall, R., Geron, C., Graedel, T., Harley, P., Klinger, L., Lerdau, M., McKay, W., Pierce, T., Scholes, B., Steinbrecher, R., Tallamraju, R., Taylor, J., and Zimmerman, P.: A global-model of natural volatile organic-compound emissions, J. Geophys. Res., 100, 8873–8892, 1995.
Guenther, A., Karl, T., Harley, P., Wiedinmyer, C., Palmer, P. I., and Geron, C.: Estimates of global terrestrial isoprene emissions using MEGAN (Model of Emissions of Gases and Aerosols from Nature), Atmos. Chem. Phys., 6, 3181–3210, doi:10.5194/acp-6-3181-2006, 2006.
Hedegaard, G. B.: Future air pollution levels in the northern hemisphere – sensitivity to climate change and projected emissions, PhD thesis, Institute of Environmental science. Aarhus University, Denmark, available at: http://www.dmu.au.dk, 2011.
Hedegaard, G. B., Brandt, J., Christensen, J. H., Frohn, L. M., Geels, C., Hansen, K. M., and Stendel, M.: Impacts of climate change on air pollution levels in the Northern Hemisphere with special focus on Europe and the Arctic, Atmos. Chem. Phys., 8, 3337–3367, doi:10.5194/acp-8-3337-2008, 2008.
Hertel, O., Christensen, J., Runge, E. H., Asman, W. A. H., Berkowicz, R., Hovmand, M. F., and Hov, Ø.: Development and Testing of a new Variable Scale Pollution model – ACDEP, Atmos. Environ., 29, 1267–1290, 1995.
Horn, H.-G., Bonka, H., and Maqua, M.: Measured particle bound activity size-distribution, deposition velocity, and activity concentration in rainwater after the Chernobyl accident, J. Aerosol Sci., 18, 681–684, 1987.
Isaksen, I. S. A., Granier, C., Myhre, G., Berntsen, T. K., Dalsøren, S. B., Gauss, M., Klimont, Z., Benestad, R., Bousquet, P., Collins, W., Cox, T., Eyring, V., Fowler, D., Fuzzi, S., Jöckel, P., Laj, P., Lohmann, U., Maione, M., Monks, P., Prevot, A. S. H., Raes, F., Richter, A., Rognerud, B., Schulz, M., Shindell, D., Stevenson, D. S., Storelvmo, T., Wang, W.-C., van Weele, M., Wild, M., and Wuebbles, D.: Atmospheric Composition Change: Climate-Chemistry interactions, Atmos. Environ., 43, 5138–5192, 2009.
Jonson, J. E., Stohl, A., Fiore, A. M., Hess, P., Szopa, S., Wild, O., Zeng, G., Dentener, F. J., Lupu, A., Schultz, M. G., Duncan, B. N., Sudo, K., Wind, P., Schulz, M., Marmer, E., Cuvelier,





ACPD
12, 4901–4939, 2012



C., Keating, T., Zuber, A., Valdebenito, A., Dorokhov, V., De Backer, H., Davies, J., Chen, G. H., Johnson, B., Tarasick, D. W., Stbi, R., Newchurch, M. J., von der Gathen, P., Steinbrecht, W., and Claude, H.: A multi-model analysis of vertical ozone profiles, Atmos. Chem. Phys., 10, 5759–5783, doi:10.5194/acp-10-5759-2010, 2010a.

Jonson, J. E., Valiyaveetil, S., Wind, P., Valdebenito, A., and Gauss, M.: Model validation of the global version of the EMEP Unified model, in: Development of the EMEP global modelling framework: Progress report, Joint MSC-W/MSC-E Report, EMEP/MSC-W Technical Report 1/2010, The Norwegian Meteorological Institute, Oslo, Norway, 14–31, 2010b.

Jylhä, K.: Empirical scavenging coefficients of radioactive substances released from Chernobyl, Atmos. Environ., 25A, 263–270, 1991.

Katragkou, E., Zanis, P., Kioutsioukis, I., Tegoulias, I., Melas, D., Krüger, B. C., and Coppola, E.: Future climate change impacts on summer surface ozone from regional climate-air quality simulations over Europe, J. Geophys. Res., 116, D22307, doi:10.1029/2011JD015899, 2011.

Kjellström, E., Nikulin, G., Hansson, U., Strandberg, G., and Ullerstig, A.: 21st century changes in the European climate: uncertainties derived from an ensemble of regional climate model simulations, Tellus 63A, 24–40, doi:10.1111/j.1600-0870.2010.00475.x, 2011.

Köble, R. and Seufert, G.: Novel Maps for Forest Tree Species in Europe, A Changing Atmosphere, 8th European Symposium on the Physico-Chemical Behaviour of Atmospheric Pollutants, Torino, Italy, 17–20 September, 2001.

Lamarque, J.-F., Bond, T. C., Eyring, V., Granier, C., Heil, A., Klimont, Z., Lee, D., Liousse, C., Mieville, A., Owen, B., Schultz, M. G., Shindell, D., Smith, S. J., Stehfest, E., Van Aardenne, J., Cooper, O. R., Kainuma, M., Mahowald, N., McConnell, J. R., Naik, V., Riahi, K., and van Vuuren, D. P.: Historical (1850–2000) gridded anthropogenic and biomass burning emissions of reactive gases and aerosols: methodology and application, Atmos. Chem. Phys., 10, 7017–7039, doi:10.5194/acp-10-7017-2010, 2010.

Langner, J., Bergström, R., and Foltescu, V.: Impact of climate change on surface ozone and deposition of sulphur and nitrogen in Europe, Atmos. Environ., 39, 1129–1141, 2005.

Logan, J. A.: An analysis of ozonesonde data for the troposphere: Recommendations for testing 3-D models, and development of a gridded climatology for tropospheric ozone, J. Geophys. Res., 104, 16115–16149, 1999.

Madronich, S. and Flocke, S.: The role of solar radiation in atmospheric chemistry, in Handbook of Environmental Chemistry, edited by: Boule, P., 1–26, Springer, New York, 1999.





ACPD
12, 4901–4939, 2012



Meleux, F., Solmon, F., and Giorgi, F.: Increase in summer European ozone amounts due to climate change, Atmos. Environ., 41, 7577–7587, doi:10.1016/j.atmosenv.2007.05.048, 2007.

Nakićenović, N., Alcamo ,J., Davis, G., de Vries, B., Fenhann, J., Gaffin, S., Gregory, K., Grübler, A., Yong Jung, T., Kram, T., La Rovere, E. L., Michaelis, L., Mori, S., Morita, T., Pepper, W., Pitcher, H., Price, L., Riahi, K., Roehrl, A., Rogner, H.-H., Sankovski, A., Schlesinger, M., Shukla, P., Smith, S., Swart, R., van Rooijen, S., Victor, N., and Dadi, Z.: Emission scenarios, A special report of working group III of the Intergovernmental Panel on Climate Change, Cambridge University Press, 2000.

Nyíri, Á., Gauss, M., Tsyro, S., Wind, P., and Haugen, J. E.: Future Air Quality, including Climate Change. In: Transboundary Acidification, Eutrophication and Ground Level Ozone in Europe in 2008, EMEP Report 1/2010, 2010.

Pacifico, F., Harrison, S. P., Jones, C. D., and Sitch, S.: Isoprene emissions and climate, Atmos. Environ., 43, 6121–6135, 2009.

Pal, J. S., Giorgi, F., Bi, X., Elguindi, N., Solmon, F., Gao, X. J., Francisco, R., Zakey, A., Winter, J., Ashfaq, M., Syed, F., Bell, J., Diffenbaugh, N., Karmacharya, J., Konare, A., Martinez-Castro, D., Porfirio da Rocha, R., Sloan, L., and Steiner, A.: Regional climate modeling for the developing world: The ICTP RegCM3 and RegCNET, B. Am. Meteorol. Soc., 88, 1395–1409, 2007.

Robertson, L., Langner, J., and Engardt, M.: An Eulerian limited-area atmospheric transport model, J. Appl. Meteor. 38, 190–210, 1999.

Roeckner, E., Brokopf, R., Esch, M., Giogietta, M., Hagemann, S., Kornblueh, L., Manzini, E., Schlese, U., and Schulzweida, U.: Sensitivity of simulated climate to horizontal and vertical resolutions in the ECHAM5 atmosphere model, J. Clim., 19, 3771–3791, doi:10.1175/JCLI3824.1, 2006.

Royal Society: Ground-level Ozone in the 21st Century: Future Trends, Impacts and Policy Implications, Science Policy Report 15/08, Royal Society, London, 2008.

Samuelsson, P., Jones, C. G., Willén, U., Ullerstig, A., Gollvik, S., Hansson, U., Jansson, C., Kjellström, E., Nikulin G., and Wyser, K.: The Rossby Centre Regional Climate model RCA3: Model description and performance, Tellus A, 63, 4–23, doi:10.1111/j.1600-0870.2010.00478.x, 2011.

Shalaby, A. K., Zakey, A. S., Tawfik, A. B., Solmon, F., Giorgi, F., Stordal, F., Sillman, S., Zaveri, R. A., and Steiner, A. L.: Implementation and evaluation of online gas-phase chemistry





ACPD
12, 4901–4939, 2012



within a regional climate model (RegCM-CHEM4), Geosci. Model Dev. Discuss., 5, 149–188, doi:10.5194/gmdd-5-149-2012, 2012.
Sillman, S.: A numerical solution for equations of tropospheric chemistry based on an analysis of sources and sinks of odd hydrogen, J. Geophys. Res., 96, 20735–20744, 1991.
Simpson, D., Andersson-Sköld, Y., and Jenkin, M. E.: Updating the chemical scheme for the EMEP MSC-W oxidant model: Current status, EMEP MSC-W Note 2/93, Norwegian Meteorological Institute, Oslo, 1993.
Simpson, D., Guenther, A. Hewitt, C. N., and Steinbrecher, R.: Biogenic emissions in Europe: 1. Estimates and uncertainties, J. Geophys. Res., 100, 22875–22890, doi:10.1029/95JD02368, 1995.
Simpson, D., Winiwarter, W., Borjesson, G., Cinderby, S., Ferreiro, A., Guenther, A., Hewitt, C. N., Janson, R., Khalil, M. A. K., Owen, S., Pierce, T. E., Puxbaum, H., Shearer, M., Skiba, U., Steinbrecher, R., Tarrason, L., and Oquist, M. G.: Inventorying emissions from nature in Europe, J. Geophys. Res., 104, 8113–8152, 1999.
Simpson, D., Fagerli, H., Jonson, J. E., Tsyro, S., Wind, P., and Tuovinen, J. P.: The EMEP Uni?ed Eulerian Model. Model Description, EMEP MSC-W Report 1/2003, Norwegian Meteorological Institute, Oslo, 2003a.
Simpson, D., Tuovinen, J. P., Emberson, L., and Ashmore, M. R.: Characteristics of an ozone deposition module II: Sensitivity analysis, Water Air Soil Pollut., 143, 123–137, doi:10.1023/a:1022890603066, 2003b.
Simpson, D., Benedictow, A., Berge, H., Bergström, R., Emberson, L. D., Fagerli, H., Hayman, G. D., Gauss, M., Jonson, J. E., Jenkin, M. E., Nyíri, A., Richter, C., Semeena, V. S., Tsyro, S., Tuovinen, J.-P., Valdebenito, Á., and Wind, P.: The EMEP MSC-W chemical transport model - Part 1: Model description, Atmos. Chem. Phys. Discuss., 12, 3781–3874, doi:10.5194/acpd-12-3781-2012, 2012.
Sitch, S., Cox, P. M., Collins W. J., and Huntingford, C.: Indirect radiative forcing of climate change through ozone effects on the land-carbon sink, Nature, 448, 791–794, doi:10.1038/nature06059, 2007.
Slinn, S. and Slinn, W.: Predictions for particle deposition on natural waters, Atmos. Environ., 12, 1013–1016, 1980.
Smith, F. B. and Clark, M. J.: The transport and deposition of radioactive debris from the Chernobyl nuclear power plant accident with special emphasis on consequences to the United Kingdom, Meteorological Office Scientific Paper, N42, HMSO, London, 1989.





ACPD
12, 4901–4939, 2012



Sofiev, M.: Extended resistance analogy for construction of the vertical diffusion scheme for dispersion models. J. Geophys. Res., 107, 4159, doi:10.1029/2001JD001233, 2002.
Sofiev, M., Siljamo, P., Valkama, I., Ilvonen, M., and Kukkonen, J.: A dispersion modelling system SILAM and it's evaluation against ETEX data, Atmos. Environ., 40, 674–685, 2006.
Sofiev, M., Galperin, M., and Genikhovich, E.: Construction and evaluation of Eulerian dynamic core for the air quality and emergency modelling system SILAM, NATO Science for peace and security Series C: Environmental Security, Air pollution modelling and its application, XIX, edited by: Borrego, C. and Miranda, A. I., Springer, 699–701, 2008.
Sofiev, M., Genikhovich, E., Keronen, P., and Vesala, T.: Diagnosing the surface layer parameters for dispersion models within the meteorological-to-dispersion modelling interface, J. Appl. Meteorol. Climatol., 49, 221–233, doi:10.1175/2009JAMC2210.1, 2010.
Sofiev, M., Soares, J., Prank, M., de Leeuw, G., and Kukkonen, J.: A regional-to-global model of emission and transport of sea salt particles in the atmosphere, J. Geophys. Res., 116, D21302, doi:10.1029/2010JD014713, 2011.
Solmon, F., Giorgi, F., and Liousse, C.: Aerosol modelling for regional climate studies: application to anthropogenic particles and evaluation over a European/African domain, Tellus B, 58, 51–72, 2006.
Strand, A. and Hov, Ø.: A two-dimensional global study of tropospheric ozone production, J. Geophys. Res., 99, 22877–22895, 1994.
Thomson, A. M., Calvin, K. V., Smith, S. J., Kyle, G. P., Volke, A., Patel, P., Delgado-Arias, S., Bond-Lamberty, B., Wise, M. A., Clarke, L. E., and Edmonds, J. A.: RCP4.5: a pathway for stabilization of radiative forcing by 2100, Climatic Change, 109, 77–94, doi:10.1007/s10584-011-0151-4, 2011.
Thunis, P., Rouil, L., Cuvelier, C., Stern, R., Kerschbaumer, A., Bessagnet, B., Schaap, M., Builtjes, P., Tarrason, L., Douros, J., Moussiolopoulos, N., Pirovano, G., and Bedogni, M.: Analysis of model responses to emission-reduction scenarios within the CityDelta project, Atmos. Environ., 41, 208–220, 2007.
Tuovinen, J.-P., Ashmore, M., Emberson, L., and Simpson, D.: Testing and improving the EMEP ozone deposition module, Atmos. Environ., 38, 2373–2385, 2004.
van Loon, M., Vautard, R. Schaap, M. Bergström, R. Bessagnet, B. Brandt, J. Builtjes, P. H. J. Christensen, J. H., Cuvelier, C., Graff, A., Jonson, J.E., Krol, M., Langner, J., Roberts, P., Rouil, L., Stern, R., Tarrason, L., Thunis, P., Vignati, E., White, L., and Wind, P.: Evaluation of long-term ozone simulations from seven regional air quality models, their ensemble, Atmos.





ACPD
12, 4901–4939, 2012



Environ., 41, 2083–2097, 2007.
Vautard, R., Builtjes, P. H. J., Thunis, P., Cuvelier, C., Bedogni, M., Bessagnet, B., Honore, C., Moussiopoulos, N., Pirovano, G., Schaap, M., Stern, R., Tarrason, L., and Wind, P.: Evaluation, intercomparison of Ozone, PM10 simulations by several chemistry transport models over four European cities within the CityDelta project, Atmos. Environ., 41, 173–188, 2007.
Vautard, R. , Schaap, M. Bergström, R., Bessagnet, B., Brandt, J., Builtjes, P.J.H., Christensen, J.H., Cuvelier, C., Foltescu, V., Graff, A., Kerschbaumer, A., Krol, M., Roberts, P., Rouïl, L., Stern, R., Tarrason, L., Thunis, P., Vignati, E., and Wind, P.: Skill and uncertainty of a regional air quality model ensemble, Atmos. Environ., 43, 4822–4832, 2009.
Vautard, R., Van Loon, M., Schaap, M., Bergström, R., Bessagnet, B., Brandt, J., Builtjes, P. J. H., Christensen, J. H., Cuvelier, C., Graff, A., Jonson, J. E., Krol, M., Langner, J., Roberts, P., Rouil, L., Stern, R., Tarrason. L., Thunis, P., Vignati, E., White, L., and Wind, P.: Is regional air quality model diversity representative of uncertainty for ozone simulation?, Geophys. Res. Lett., 33, L24818, doi:10.1029/2006GL027610, 2006.
Vieno, M., Dore, A. J., Stevenson, D. S., Doherty, R., Heal, M. R., Reis, S., Hallsworth, S., Tarrason, L., Wind, P., Fowler, D., Simpson, D., and Sutton, M. A.: Modelling surface ozone during the 2003 heat-wave in the UK, Atmos. Chem. Phys., 10, 7963–7978, doi:10.5194/acp-10-7963-2010, 2010.
Wesely, M. L.: Parameterization of surface resistance to gaseous dry deposition in regional-scale numerical models, Atmos. Environ., 23, 1293–1304, 1989.
Zaveri, R. and Peters, L. K.: A new lumped structure photochemical mechanism for large-scale applications, J. Geophys. Res., 104, 30387–30415, 1999.
Zhang, L. Moran, M. D., Makar, P. A., Brook, J. R., and Gong, S.: Modelling gaseous dry deposition in AURAMS: a unified regional air-quality modelling system, Atmos. Environ., 36, 537–560, 2002.
Zhang, L., Brook, J. R., and Vet, R.: A revised parameterization for gaseous dry deposition in air-quality models, Atmos. Chem. Phys., 3, 2067–2082, doi:10.5194/acp-3-2067-2003, 2003.
Zhang, Y.: Online-coupled meteorology and chemistry models: history, current status, and outlook, Atmos. Chem. Phys., 8, 2895–2932, doi:10.5194/acp-8-2895-2008, 2008.





ACPD
12, 4901–4939, 2012



**Table 1.** Average annual biogenic emissions of isoprene in models.

| Model | Emission (Gg $yr^{-1}$) 2000–2009 | Emission (Gg $yr^{-1}$) 2040–2049 |
|---|---|---|
| DEHM | 8018 | 9910 |
| EnvClimA | Offline | Offline |
| EMEP | 3405 | 4114 |
| SILAM | Not available* | Not available* |
| MATCH | 1592 | 1917 |

* Isoprene emissions were not stored for analysis.





ACPD
12, 4901–4939, 2012



**Table 2.** Model characteristics.

| Model | Type | Horizontal grid | Lowest model layer (m) | Model top (km) | #levels | Meteorological input data |
|---|---|---|---|---|---|---|
| DEHM | Eulerian/Offline | 150 km × 150 km polar stereographic | 60 | 16 | 20 | ECHAM5-r3 (global data) |
| EnvClimA | Eulerian/online | 50 km × 50 km Lambert | 50 | 20 | 18 | ECHAM5-r3 – RegCM4 |
| EMEP | Eulerian/Offline | 0.44° × 0.44° rotated latitude longitude | 90 | 16 | 20 | ECHAM5-r3 – RCA3 |
| SILAM | Eulerian/Offline | 0.44° × 0.44° rotated latitude longitude | 50 | 10 | 9 | ECHAM5-r3 – RCA3 |
| MATCH | Eulerian/offline | 0.44° × 0.44° rotated latitude longitude | 60 | 5.5 | 15 | ECHAM5-r3 – RCA3 |





ACPD
12, 4901–4939, 2012



**Table 3.** Statistical evaluation of model results for surface $O_3^*$.

| | Annual mean | AMJJAS mean | Annual daily max | AMJJAS daily max |
|---|---|---|---|---|
| | | Mean ppb(v) | | |
| Observations | 30.8 | 36.4 | 41.6 | 49,6 |
| DEHM | 28.9 | 34.2 | 34.5 | 40.1 |
| EnvClimA | 24.6 | 34.0 | 30.3 | 41.1 |
| EMEP | 36.1 | 42.4 | 42.4 | 49.0 |
| SILAM | 38.6 | 44.8 | 43.0 | 50.1 |
| MATCH | 31.4 | 37.3 | 39.9 | 45.4 |
| | | Bias % | | |
| DEHM | −2.9 | −5.5 | −16.9 | −19.2 |
| EnvClimA | −20.2 | −6.7 | −27.2 | −17.1 |
| EMEP | 17.3 | 16.5 | 2.0 | −1.1 |
| SILAM | 25.4 | 23.1 | 3.5 | 1.1 |
| MATCH | 2.1 | 2.3 | −3.9 | −8.4 |
| | | Spatial correlation | | |
| DEHM | 0.53 | 0.64 | 0.67 | 0.84 |
| EnvClimA | 0.60 | 0.78 | 0.79 | 0.90 |
| EMEP | 0.43 | 0.69 | 0.67 | 0.85 |
| SILAM | 0.21 | 0.65 | 0.68 | 0.89 |
| MATCH | 0.56 | 0.63 | 0.68 | 0.82 |
| # stations | 59 | 63 | 59 | 61 |

* Model results are for lowest model level. Observations are for the period 1997–2003. Sites at an elevation deviating more than 250 m from the model height or with a data capture less than 90 % and five years were excluded from the evaluation. Results for EnvClimA are based on 6-hourly data.





ACPD
12, 4901–4939, 2012



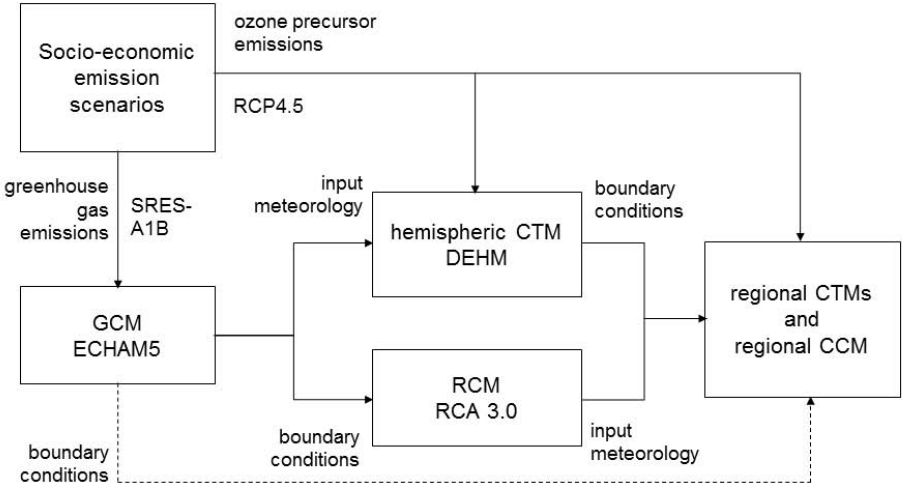


**Fig. 1.** Model chain used in the study.





ACPD
12, 4901–4939, 2012



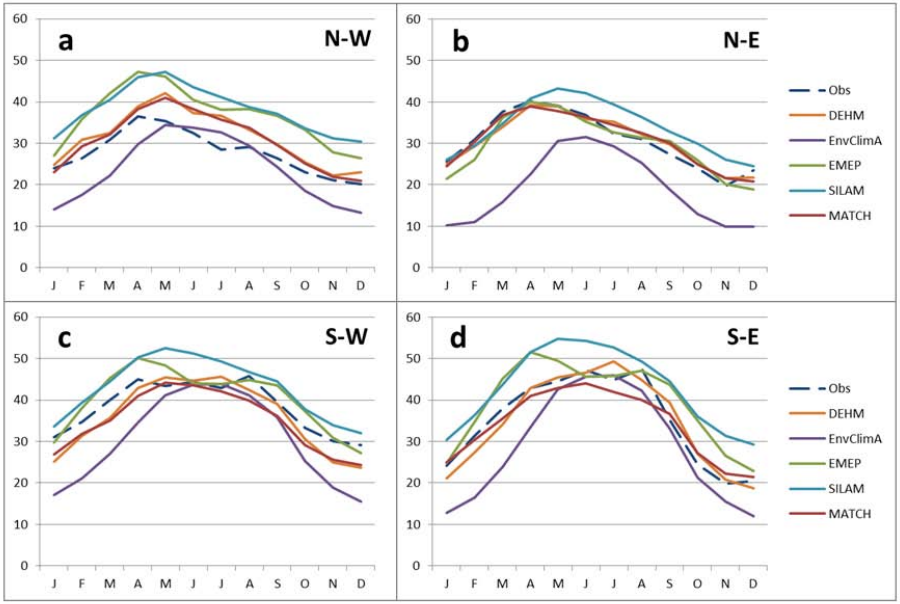


**Fig. 2.** Model simulated and observed seasonal cycle of monthly average surface $O_3$ concentrations for each quadrant of the simulation domain. Observations are averages for the period 1997–2003 and for stations indicated in Fig. 4. The number of stations in each quadrant is **(a)** 24,**(b)** 27, **(c)** 18 and **(d)** 12. Model results are for the reference period, 2000–2009, using meteorology from each CTM's driving climate model (ECHAM5-r3, ECHAM5-r3-RegCM4 and 3 × ECHAM5-r3-RCA3), and are from lowest model layer, ca. 25–45 m height. Units ppb(v).





ACPD
12, 4901–4939, 2012



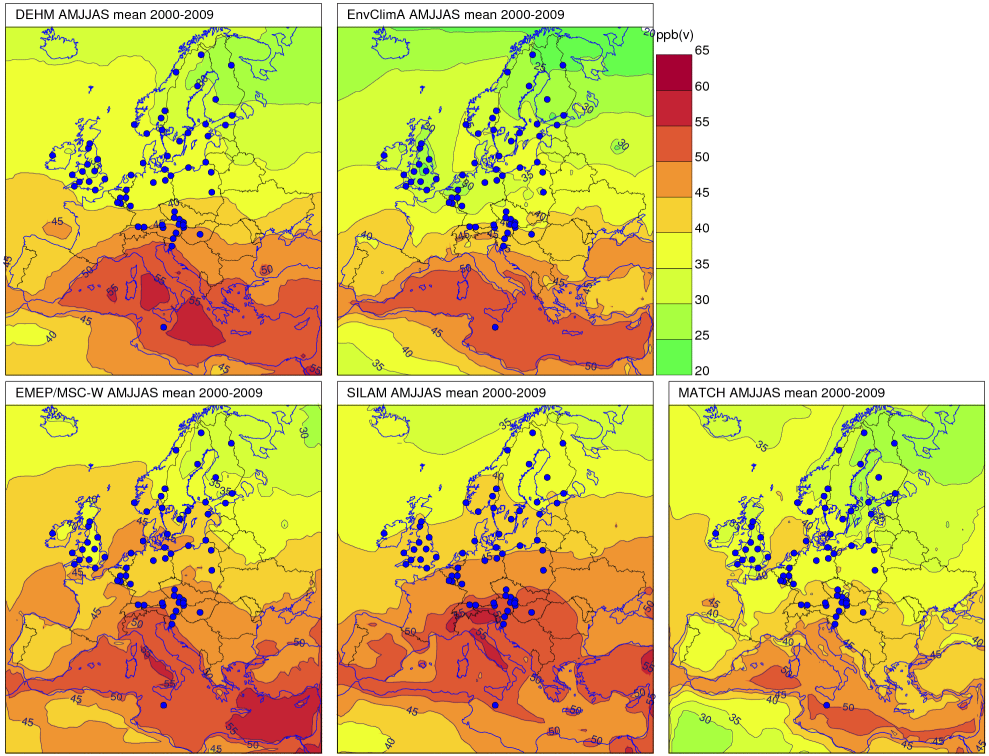


**Fig. 3.** Simulated April–September average $O_3$ concentration at the lowest model level for the period 2000–2009. Blue dots indicate locations of stations used in the model evaluation given in Table 3. Units ppb(v).





ACPD
12, 4901–4939, 2012



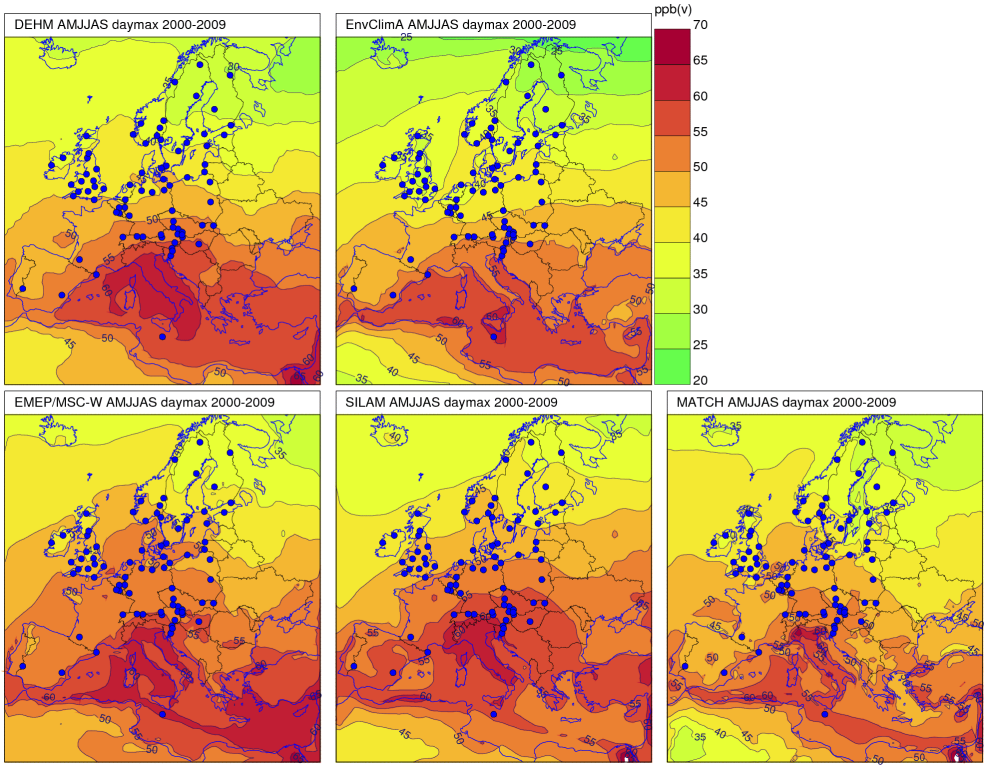


**Fig. 4.** Simulated April–September average daily maximum $O_3$ concentration at the lowest model level for the reference period, 2000–2009. Blue dots indicate locations of stations used in the evaluation of seasonal variation given in Fig. 2. Units ppb(v).





ACPD
12, 4901–4939, 2012



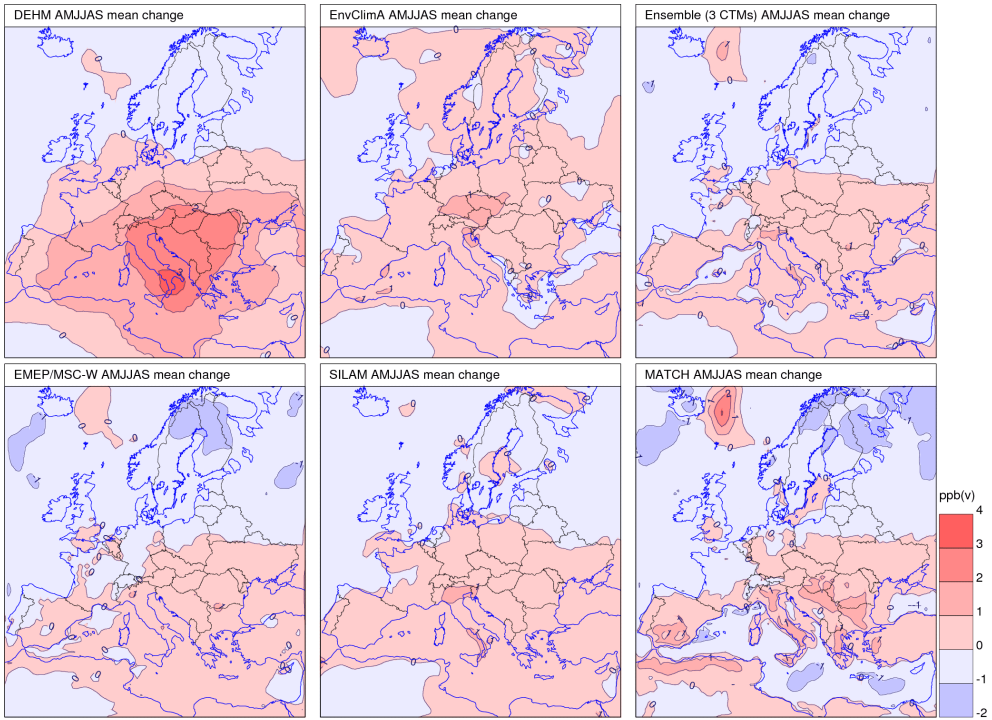


**Fig. 5.** Simulated April–September change 2000–2009 to 2040–2049 in average $O_3$ concentration at the first model level. Units ppb(v).





ACPD
12, 4901–4939, 2012



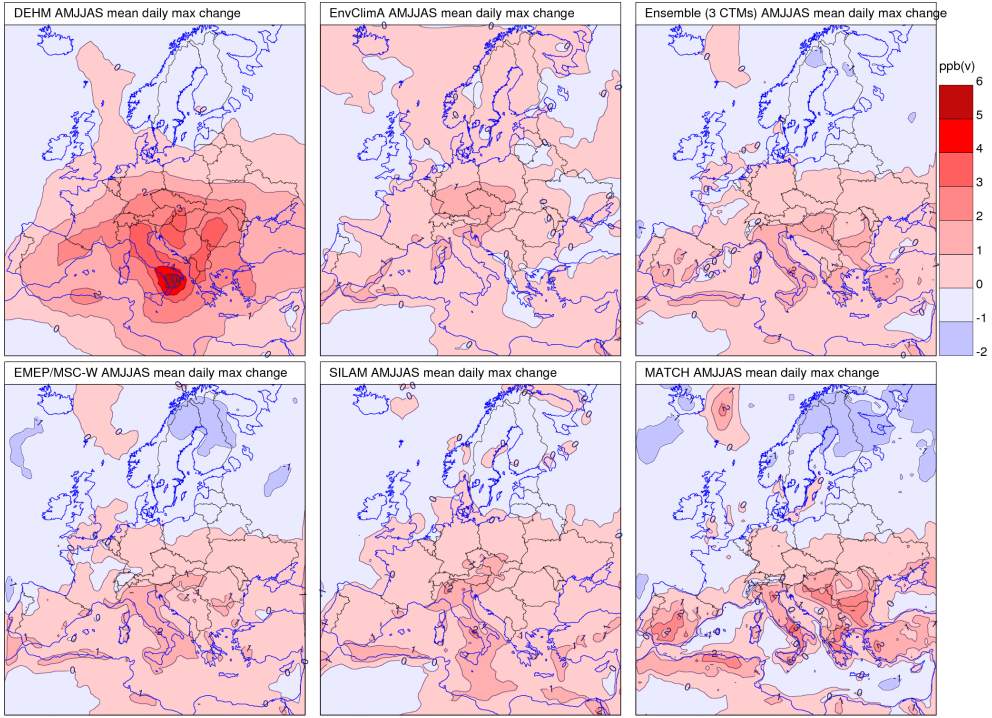


**Fig. 6.** Simulated April–September change 2000–2009 to 2040–2049 in average daily maximum $O_3$ concentration at the first model level. Units ppb(v).





ACPD
12, 4901–4939, 2012



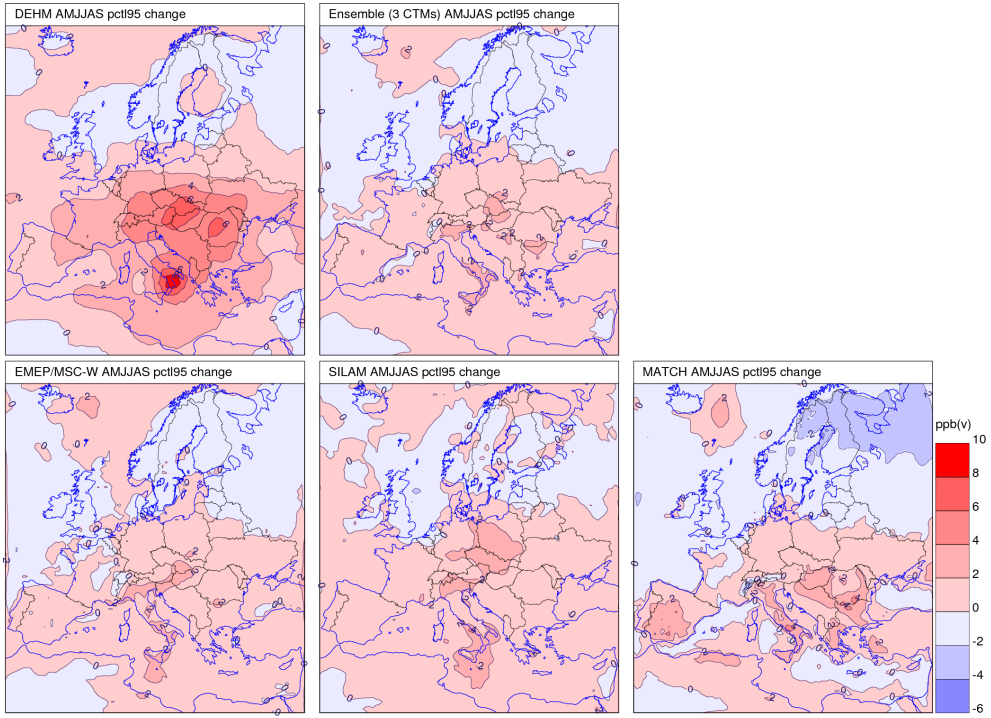


**Fig. 7.** Simulated April–September change 2000–2009 to 2040–2049 in 95-percentile $O_3$ concentration at the first model level. Units ppb(v).





ACPD
12, 4901–4939, 2012